Available online at www.sciencedirect.com
SCIENCE DIRECT®

Journal of the European Ceramic Society 24 (2004) 2717–2722
www.elsevier.com/locate/jeurceramsoc

Flocculation and coagulation kinetics of Al_2O_3 suspensions

Jens Cordelair*, Peter Greil

Friedrich Alexander University of Erlangen—Nuremberg, Department of Materials Science (Glass and Ceramics), Martensstr. 5, 91058 Erlangen, Germany

Received 15 January 2003; received in revised form 25 August 2003; accepted 30 August 2003

Abstract

The effect of solid content on the structure of Al_2O_3 particle networks is studied by Brownian dynamics simulations using a novel interaction potential with image charges. Significant differences between 1 and 2 vol% suspensions are discussed with pair correlation functions, particle coordination numbers and cluster sizes. It is concluded, that the 2 vol% system is nearer to the percolation limit, thus fast aggregation occur. It is also stated, that the clustering dynamics should be described rather by the flocculation half-life than by the coagulation half-life. In real particle systems the interaction energy is not conservative due to friction with the medium. New expressions for the flocculation and coagulation half-life are derived using the interaction force as determining parameter, without the need for energy conservation. The corresponding coagulation half-life is compared with the classical expression of Fuchs.

Keywords: Al_2O_3; Flocculation; Simulation; Suspensions

1. Introduction

Ceramics have been processed by colloidal routes for the several millennia since clay based pottery was invented. Unreliability is perhaps the greatest barrier to wider use of ceramic products. It is known, that this unreliability is related to variations in defect size within the ceramic microstructure. Colloidal powder processing offers the potential to produce ceramic materials and products with improved microstructure homogeneity.[1]

It has been shown that agglomerates are a major limiting factor for high strength and Weibull modulus of ceramics made by sintering.[2] Lange and coworkers[3] proposed a new paradigm for powder processing. Their approach embodied many principles including the use of powders with controlled size, morphology, purity and dispersion control. Specifically, the colloidal system was first prepared in a dispersed state to effectively eliminate powder agglomerates, an important source of unwanted defects. The system was then adjusted to a weakly flocculated state to create the desired plasticity needed for the forming process.

Destabilization of a colloidal suspension leads to the formation of larger units, which range from loose flocs at low solid content to percolating particle networks at higher solid loads. The effect of solid content and colloidal interactions on the structure of the colloid network can be studied by Brownian dynamics simulations. It has been shown, that a high solid content results in a freezing like transformation of the initial liquid suspension structure, and that this effect can be reduced by introducing a shallow secondary minimum[4] in the interaction potential. However, the structures resulting from such slow coagulation show a substantial degree of porosity, higher than those produced at the same solid content but by fast coagulation.

In the present work, characteristic coagulation time scales in colloidal suspensions have been identified using Brownian dynamics simulation techniques and their dependence on solid load and interaction potential have been measured.[5]

2. Experimental procedure

A submicron Al_2O_3 ceramic powder (Table 1) was used to determine the parameters for the simulation. Measurements of the Zeta potential vs. pH by means of

* Corresponding author.
E-mail address: jens.cordelair@freenet.de (J. Cordelair).

0955-2219/$ - see front matter © 2003 Elsevier Ltd. All rights reserved.
doi:10.1016/j.jeurceramsoc.2003.08.014

Table 1
Particle properties

	Al_2O_3 (Alcoa)
Mean particle size [μm]	0.8
Zeta potential pH 4 [mV]	85
Isoelectric point [pH]	7.8
Hamaker constant [10^{-20} J]	3.67

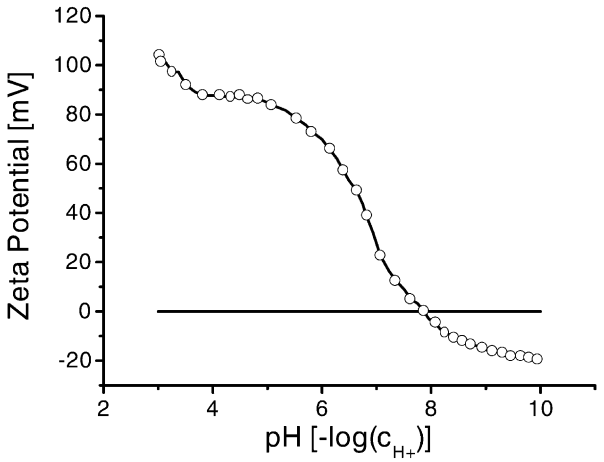

Fig. 1. Zeta potential of Al_2O_3.

the electrokinetic sonic amplitude technique (ESA 9800, Matec, Northborough, USA) showed that the Al_2O_3 powder had an isoelectric point at $pH_{iep} \approx 7.8$ and a maximum zeta potential of 88 mV below pH 5. The maximum negative zeta potential of −20 mV was found at pH 10 (Fig. 1).

2.1. Brownian dynamics simulation

The theory of Brownian motion has been developed to describe the dynamic behavior of particles whose mass and size are much larger than those of the host medium. Due to the large mass and size of the Brownian particles, the distribution of momenta relaxes to the equilibrium distribution much more rapidly than does the distribution of particle positions.[6] Physically this occurs as a result of many collisions which the particle has with the surrounding fluid particles. The distribution of momenta essentially reaches the equilibrium distribution before the positions of the Brownian particles have changed significantly.

Consequently the motion of the particles in the fluid can be subdivided into two parts. The first part, we call friction, occurs when the particles interact with each other or with external force fields. During the interaction the frictional force balances the applied force. According to Stokes law the velocity is proportional to the frictional force of the particle

$$\frac{\mathrm{d}\vec{x}}{\mathrm{d}t} = \frac{D_0}{kT} \cdot \vec{F} \tag{1}$$

where $D_0 = \frac{kT}{6\pi a\eta}$ is the diffusion coefficient of the particle, a the particle radius, η the dynamic viscosity of the fluid and $\vec{F}$ the force acting on the particle.

As second part of the fluid–particle interaction a stochastical displacement $\vec{R}$ is present which follows a normal distribution with mean and variance[6]

$$\left\langle \vec{R} \right\rangle = 0 \; ; \; \left\langle R_i^2 \right\rangle = 2D_0\Delta t. \tag{2}$$

Numerically the positions of the particles can be calculated according to the iteration scheme

$$\vec{x}^{k+1} = \vec{x}^{k} + \frac{D_0}{kT}\vec{F} \cdot \Delta t + \vec{R}. \tag{3}$$

This is the equation of motion, which was solved for short time intervals Δt ($\sim 10^{-8}$ s) for 128 particles under a new interaction force with image charges. The normal distribution for the random displacement was generated using the random generator normal distribution of the free boost C^{++} library (http://www.boost.org).

3. Numerical solution for the double layer with image charges

The method of image charges can be used to solve electrostatic problems, where charges are near to boundaries under constant potential or charge.[7] Under good geometrical conditions (planes, spheres…) the boundary condition for the border surface can be satisfied by placing charges of suitable size into the territory which is not under consideration. These charges are called image charges. They substitute the real problem of the boundary condition on the surface by enlarging the region which has to be taken into consideration with image charges without boundary condition. The boundary condition is fulfilled due to the presence of the image charges.

The differential equation for the potential curve with image charges for spherical particles with radius a reads[8]

$$\Delta\psi_{(r)} = -\frac{4\pi}{\varepsilon}\left(1 - \frac{a^7}{r^7}\right)\rho_{(r)}. \tag{4}$$

Starting from the surface of a spherical particle the run of the potential can be calculated numerically by successive summation about charged shells. The potential at the outer Helmholz layer, the zeta potential ζ, can be derived from experimental measurements. This value for the potential on the surface of the particle is taken to initialize the sequential integration for the run of the potential in the diffuse part of the double layer.

The value of the charge density ρ may be obtained directly from Bolzmann's theorem as it is given by the local excess of ions of one sign. In order to simplify the formula we will introduce the restriction of considering only solutions containing ions of one valance v and we therefore write $v_n = v_p = v$. The charge density may then be written as

$$\rho = ve\left(n_p \exp\left(\frac{-ve\psi}{kT}\right) - n_n \exp\left(\frac{ve\psi}{kT}\right)\right)$$
$$= -2n \text{ ve } \sinh\left(\frac{ve\psi}{kT}\right) \quad (5)$$

where n_p and n_n are the concentrations of positive and negative ions at large distances from the surface.

A good approximation for the charge of a colloidal particle can be derived from

$$Q = C_{spec} \cdot A \cdot \zeta \quad (6)$$

where $C_{spec} = \frac{C}{A} = 5 \cdot 10^{18} \cdot n^{0,44}$ is the specific capacitance in aqueous solutions and A the surface area of the particle.[8]

4. Interactions in colloidal systems

The interaction energy of two particles with respect to each other, as far as the interaction of the double layers is concerned, can be determined from the free energy of the system of two double layers as a function of the distance. The interaction potential under non-equilibrium conditions can be derived from the potential that particle I induces on the surface of particle II. For equal particles the electrostatic pair potential reads

$$V_R = Q(\psi_d - \psi_\infty) = Q_{II}\psi_I^{eff} = \frac{Q_{II}\int_{S_2}\psi_I dS_2}{\int_{S_2} dS_2}. \quad (7)$$

The integral can be solved numerically, when the potential curve ψ_I of particle I is known.[8] The potential curve of a free particle gives a valuable upper limit for ψ_I; thus the electrostatic interaction potential can be calculated numerically.

Hamaker showed how the attractive London–Van der Waals interaction between two spherical particles may be found from the interaction between the molecules of these spheres. His expression for the interaction energy is

$$V_{vdW} = -\frac{H}{6}\left[\frac{2a_1a_2}{h^2 + 2h(a_1+a_2)} + \frac{2a_1a_2}{h^2 + 2h(a_1+a_2) + 4a_1a_2} + \ln\left(\frac{h^2 + 2h(a_1+a_2)}{h^2 + 2h(a_1+a_2) + 4a_1a_2}\right)\right] \quad (8)$$

where H is the Hamaker constant.[9]

The force between the particles can be calculated from the total interaction potential $V_{total} = V_{electrostatic} + V_{vdW}$ according to

$$\vec{F} = -\vec{\nabla} V_{total}. \quad (9)$$

Fig. 2 shows the forces between Al_2O_3 particles at different pH, with an additional ion concentration c_0 of $3.2 \cdot 10^{-4}$ mol/l.

5. Results

Fig. 3 shows the particle configurations of a suspension with a particle concentration of 1 vol% at pH 4 with an additional ion concentration of $3.2 \cdot 10^{-4}$ mol/l during the flocculation process. Starting from a well dispersed state, the particles rapidly flocculate, thus after 2 s small clusters are formed. These small clusters grow at the cost of single particles, until after ca. 10 s only a few particles remain separated. After 20 s the clusters have grown to their stable maximum size. Further growth of particle clusters is suppressed due to the immobility of the remaining large clusters.

The pair correlation function $g_{(r)}$ gives the frequency that any two particles in the system are separated by the distance r. The structural order of the suspension can be identified by discrete peaks in the correlation function. Fig. 4 shows the correlation function of a suspension with a particle load of 5 vol% after 30 s. At least five discrete peaks can be identified.

Fig. 5 shows the time dependence of the frequency of the fourth peak (1,99 d_{min}) in the correlation function for different particle concentrations. In the dilute regime, with particle concentrations below 1 vol%, the frequency increases moderate with time. At higher particle concentrations a strong increment occur at the beginning until saturation is reached. Especially the

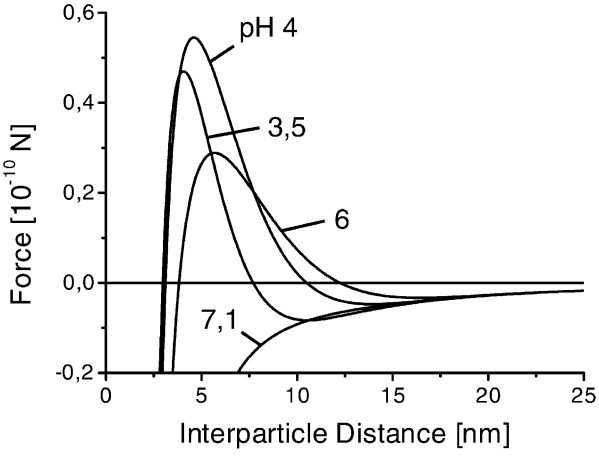

Fig. 2. Interaction force of Al_2O_3 particles with an additional ion concentration of $3.2 \cdot 10^{-4}$ mol/l.

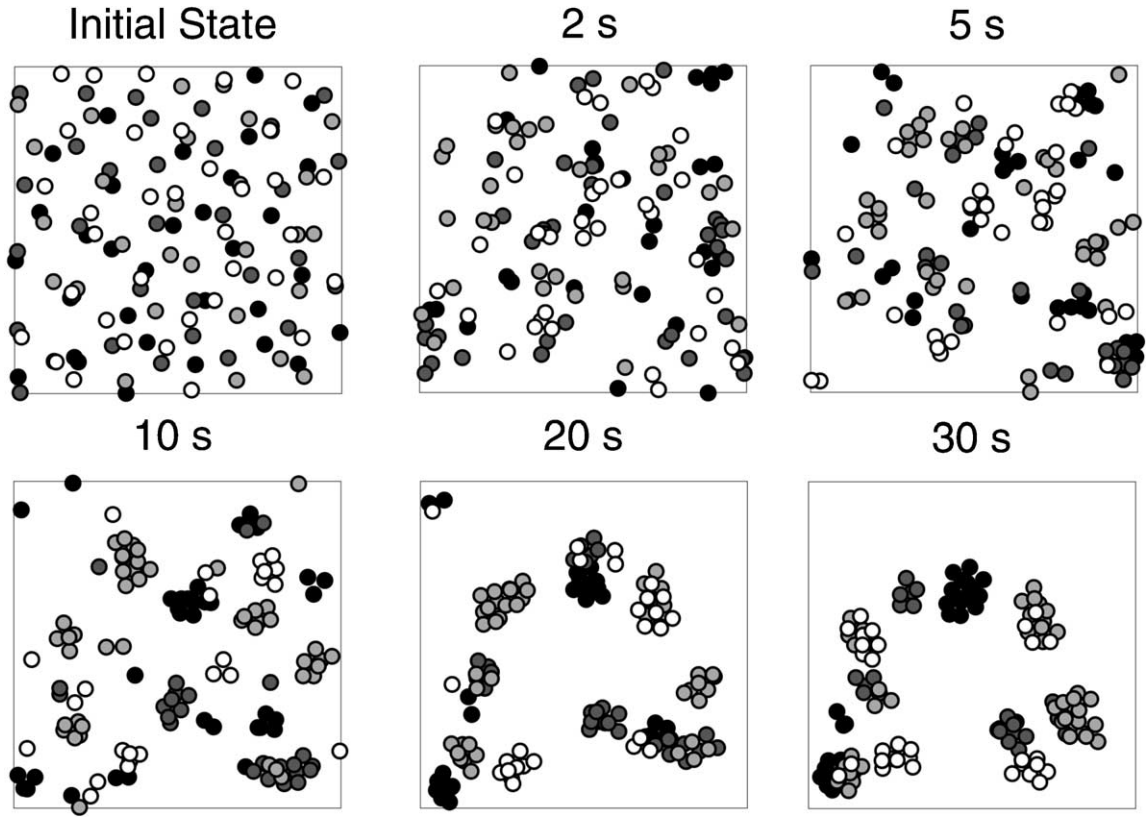

Fig. 3. Time dependence of the configuration of an Al_2O_3 suspension at pH 4 with 1 vol% particle load.

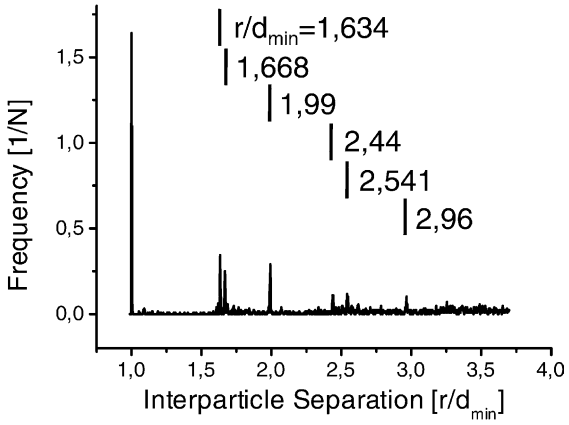

Fig. 4. Pair correlation function after 30 s of a 5 vol% Al_2O_3 suspension.

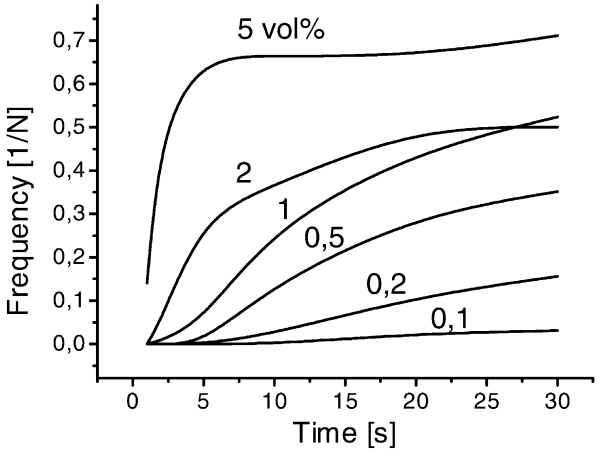

Fig. 5. Time dependence of the 1.99 peak of the correlation function for different particle loads.

particle concentrations 1 and 2 vol% show an interesting crossover region at around 30 s, where the peak of the 1 vol% system becomes higher than that of the 2 vol% system.

6. Discussion

The coordination numbers of the particles (number of nearest neighbors; Fig. 4, peak 1,0) show significant differences between the particle systems with 1 vol% (Fig. 6a) and 2 vol% (Fig. 6b). While the 1 vol% system remains dispersed after 1 up to 5 s with only minor interconnections, the 2 vol% system begins to flocculate immediately. The smaller mobility of the flocs will hinder further flocculation until the coordination numbers of the 1 vol% system have shifted to larger numbers after 30 s.

The cluster size (number of particles in a cluster, Fig. 7) shows that after 5 s a lot of particles in the 1 vol% system remain as single particles or pairs and

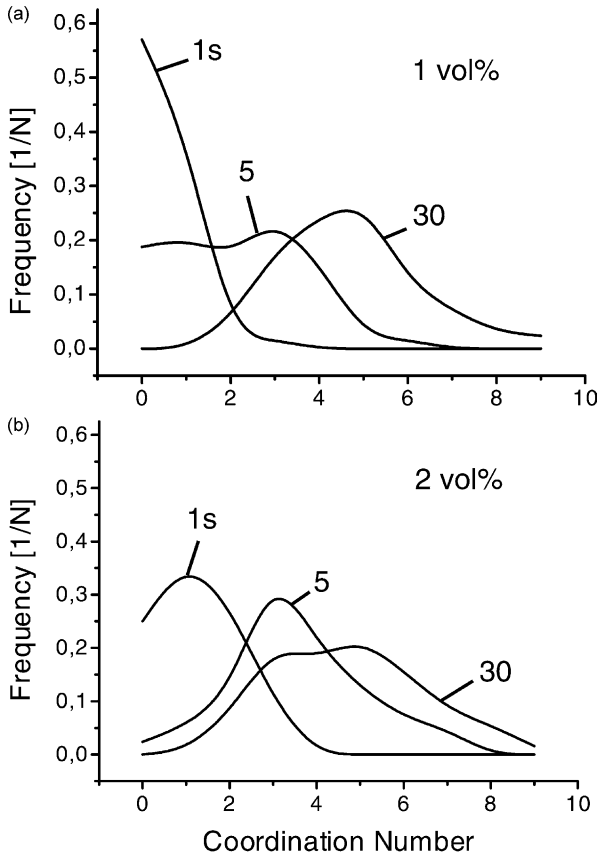

Fig. 6. Coordination numbers with particle load (a) 1 vol%, (b) 2 vol%.

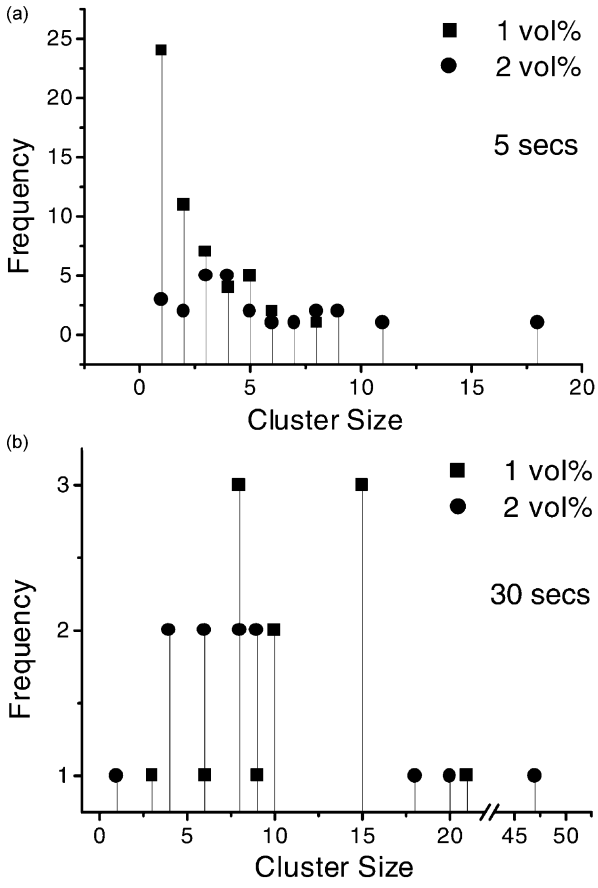

Fig. 7. Cluster size distribution after (a) 5 s, (b) 30 s.

some are clustered in small flocs with 5–7 particles after 5 s. Only few larger clusters exist. In the system with 2 vol%, there are only few single particles or pairs, and some small flocs with particle size of 5–7 are present. More than half of all particles are bound in larger flocs.

After 30 s no single particles or pairs are present in either system (Fig. 7b) and half of the particles are bound in flocs smaller than 10 particles, but in the system with 1 vol% three clusters exist with 15 and one with 21 particles, while in the system with 2 vol% two clusters around 20 particles and one large cluster with 44 particles exist. At lower solid contents the particles have to move longer distances before they sense the existence of other particles through the attractive interaction force. When the particle concentration is high enough, each particle will sense at least one other particle, thus flocculation will start immediately and fast flocculation will appear. The 2 vol% system is near to the percolation threshold, and flocculation immediately starts, while the 1 vol% system persists in the dispersed state for longer. In the system with 5 vol%, the percolation threshold may be crossed, because only 2 large clusters exist with 99 and 29 particles after 30 s.

In our investigations we found that no coagulation was present, when the interaction potential barrier was larger than kT, no matter if it was of negative value. In

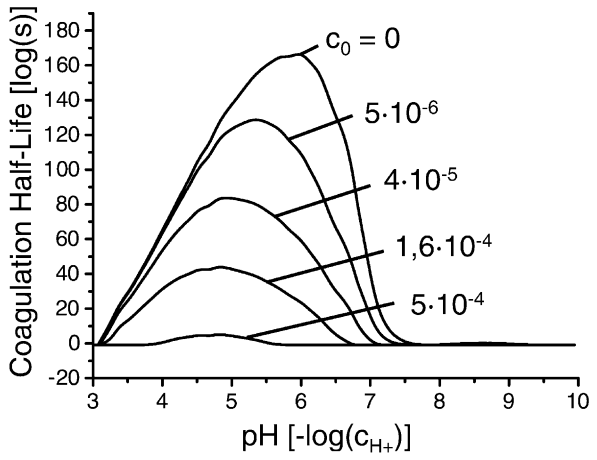

Fig. 8. Modified coagulation half-life.

practice there is no parameter set, where flocculation can be avoided, thus the main influence of the interaction potential was to define the equilibrium separation through the location of the potential minimum d_{min}.

A colloidal dispersion is called stable when the dispersed particles essentially remain as discrete, single particles on a long time scale. Electric double-layer repulsion and London–van der Waals attraction allow a quantitative description of the stability of colloidal

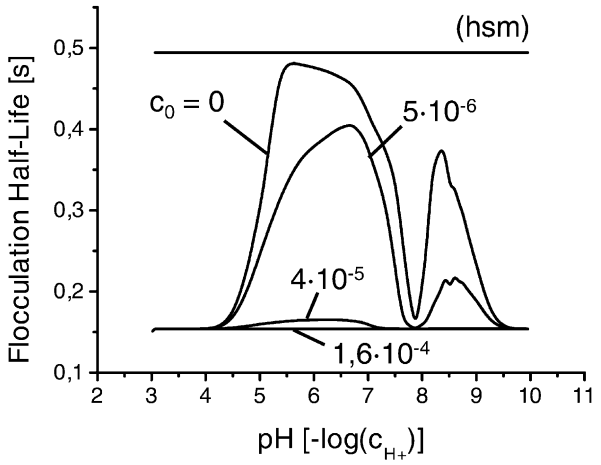

Fig. 9. Flocculation half-life.

systems. From the total energy curves, it is possible to derive a criterion for the stability of colloids, the coagulation half-life. Fuchs[10] described how the coagulation half life can be found from

$$T_{\frac{1}{2}} = \frac{1}{8\pi D_0 a n} \cdot 2a \int_{2a}^{\infty} \exp\left(\frac{V_{\text{tot}}}{kT}\right) \frac{\mathrm{d}r}{r^2}. \tag{10}$$

The interaction between the particles is not conservative, thus energy is lost during the interaction and the interaction force may be a better criterion to describe the coagulation and flocculation half-life. Dividing the force into an attractive and repulsive part by

$$\begin{aligned} &\vec{F}^{+} = \vec{F} \text{ if } \vec{F} \text{ is repulsive} \\ &\vec{F}^{+} = 0 \text{ else} \end{aligned} \tag{11a}$$

and

$$\begin{aligned} &\vec{F}^{-} = \vec{F} \text{ if } \vec{F} \text{ is attractive} \\ &\vec{F}^{-} = 0 \text{ else} \end{aligned} \tag{11b}$$

we can define the repulsive V_{tot}^{+} and attractive V_{tot}^{-} interaction potentials by

$$V_{\text{tot}(r)}^{+} = \int_{\infty}^{r} \left| \vec{F}^{+} \right| \mathrm{d}r \tag{12a}$$

$$V_{\text{tot}(r)}^{-} = -\int_{\infty}^{r} \left| \vec{F}^{-} \right| \mathrm{d}r. \tag{12b}$$

In analogy to the coagulation half-life according to Fuchs, the modified coagulation and flocculation half-life can be found from

$$T_{\frac{1}{2}}^{\text{coa}} = \frac{1}{8\pi D_0 a n} \cdot 2a \int_{2a}^{\infty} \exp\left(\frac{V_{\text{tot}(r)}^{+}}{\mathrm{k}T}\right) \frac{\mathrm{d}r}{r^2} \tag{13a}$$

$$T_{\frac{1}{2}}^{\text{floc}} = \frac{1}{8\pi D_0 a n} \cdot 2a \int_{2a}^{\infty} \exp\left(\frac{V_{\text{tot}(r)}^{-}}{kT}\right) \frac{\mathrm{d}r}{r^2}. \tag{13b}$$

The Al_2O_3 system with particle concentration $n = 2$ vol% shows a wide range where the modified coagulation half life is large up to $c_0 = 2 \cdot 10^{-4}$ mol/l (pH 3.3–7) thus the suspension is essentially stable (Fig. 8). Above pH 7 the suspension is not stable. The deviation from the corresponding coagulation half-life according to Fuchs is small.

The flocculation half-life (Fig. 9) of the Al_2O_3 system is also at very low additional ion concentrations c_0 below the flocculation half-life of hard spheres (hsm), thus flocculation can't be prevented.

7. Conclusion

It has been shown that Al_2O_3 is essentially stable against coagulation in the pH regime from 3.3–7, when the concentration of additional ions is below $c_0 = 2 \cdot 10^{-4}$ mol/l but that the structure formation during Brownian dynamics aggregation must be described by the flocculation half-life.

Particle densities larger than 1 vol% have been shown to result in large flocculated clusters and the percolation threshold was assumed to be below 5 vol%. For colloidal processes, where a dispersed suspension is needed, the particle concentration must be below 1 vol%, to eliminate larger flocs.

References

1. Lewis, J. A., Colloidal processing of ceramics. *J. Am. Ceram. Soc.*, 2000, **83**(10), 2341.
2. Kendall, K., McNAlford, N., Clegg, W. J. and Birchall, J. D., High strength and Weibull modulus from colloidal processing of ceramics. In *Brit. Ceram. Proc., Fabrication Technology*, ed. R. W. Davidge and D. P. Thompson. The Institute of Ceramics Shelton, Stoke-on-Trent, UK, 1990.
3. Lange, F. F., Powder processing science and technology for increased reliability. *J. Am. Ceram. Soc.*, 1989, **72**(1), 3–15.
4. Hütter, M., Local structure evolution in particle network formation studied by Brownian dynamics simulations. *J. Coll. Interface Sci.*, 2000, **231**, 337–350.
5. Nüβer, W., *Computersimulationen kolloidaler Suspensionen*, PhD Theses, TH-Aachen, (in German), 1996.
6. Ermak, D. L. and McCammon, J. A., Brownian dynamics with hydrodynamic interactions. *J. Chem. Phys.*, 1978, **69**(4), 1352–1360.
7. Jackson, J. D., *Classical Electrodynamics*. Wiley/VCH, Weinheim (Germany), 1998.
8. Cordelair, J. and Greil, P., Application of the method of images on electrostatic phenomena in aqueous Al_2O_3 and ZrO_2 suspensions. *J. Coll. Interface Sci.*, 2003, **265**(2), 359–371.
9. Israelachvili, J. N., *Intermolecular and Surface Forces*. Academic Press, London, 1995.
10. Fuchs, N., Über die Stabilität und Aufladung der Aerosole. *Z. Phys.*, 1934, **89**, 736.